Quantum test of the Lorenz condition

Renato Vieira dos Santos
Instituto de Ciência, Tecnologia e Inovação – ICTIN, Universidade Federal de Lavras – UFLA, Campus Paraíso, MG 37950-000, Brazil
E-mail: `renato.santos@ufla.br`

The time-dependent electric Aharonov-Bohm effect, where shielded potentials vary while electrons are in transit, offers a unique test of the Lorenz condition $\partial_\mu A^\mu = 0$. We introduce a phenomenological coupling κ between the scalar $\partial_\mu A^\mu$ and the electron. In the field-free interior of shielded cylinders, $\partial_\mu A^\mu = \dot{\Phi}/c^2$, giving an additional phase $\Delta\phi_{\mathcal{B}} = -\kappa[\Delta V(T) - \Delta V(0)]$. For sinusoidal modulation this yields a $1-\cos(\omega T)$ term orthogonal to the standard $\sin(\omega T)$ Aharonov-Bohm phase. We propose a realistic electron interferometer, analyse fringe-field systematics, and project a sensitivity $|\kappa| \sim 10^{-6}\,\mathrm{V}^{-1}$, the first such probe. A null result would confirm the scalar mode's decoupling from matter; a positive signal would uncover a new electromagnetic degree of freedom.

Keywords: Time-dependent electric Aharonov-Bohm effect; Lorenz condition; Scalar electrodynamics; Electron interferometry; Gauge invariance; Quantum phase shift

1. Introduction

In their seminal 1959 paper, Aharonov and Bohm [1] predicted that electrons traversing regions free of electric and magnetic fields can accumulate measurable phase shifts due to electromagnetic potentials. The magnetic version has been confirmed with high precision [2,3,4], but the original electric proposal—two shielded conducting cylinders driven by time-dependent potentials—has never been realised. Standard quantum mechanics predicts a phase difference

$$\Delta\phi_{\mathrm{QM}} = -\frac{e}{\hbar}\int_0^T \big[\Phi_1(t) - \Phi_2(t)\big]\,dt, \tag{1}$$

whose functional dependence on the temporal profile of the potential remains unmeasured. The only related experiment, the steady-state Matteucci-Pozzi effect [5], was later shown to be dominated by classical forces [6]. The genuine time-dependent electric AB effect therefore constitutes an open empirical frontier.

Beyond completing the AB programme, this configuration offers a rare opportunity to interrogate a foundational tenet of electrodynamics: the status of the Lorenz condition

$$\mathcal{B} \equiv \partial_\mu A^\mu = \nabla\cdot\mathbf{A} + \frac{1}{c^2}\frac{\partial\Phi}{\partial t}. \tag{2}$$

In standard electrodynamics, local $U(1)$ gauge invariance renders the four-potential redundant; the Lorenz condition $\mathcal{B} = 0$ is a convenient gauge choice that decouples the scalar and longitudinal modes from observables. However, the question of whether this decoupling is an exact dynamical requirement or whether a small residual coupling could exist—as suggested, for instance, by emergent gauge theories [7,8] where gauge symmetry is only approximate—has never been subjected to direct experimental test in a regime where the fields vanish while the potentials vary in time. In essence, the shielded electron interferometer serves as a **quantum probe of the scalar sector**, converting a temporal boundary difference into a measurable phase shift with shot-noise-limited precision.

We address this question by adopting a strictly phenomenological approach. We do not commit to any specific modified electrodynamics; we simply posit that, if $\mathcal{B}$ has physical content, an electron might experience an additional interaction proportional to it. We further assume that any such interaction is weak enough not to alter the standard solution of the screened AB configuration at leading order. Inside the conducting cylinders, Maxwell's equations then still give $\mathbf{E} = \mathbf{B} = 0$ and a uniform potential $\Phi(t)$, so that $\mathcal{B} = \dot{\Phi}/c^2$. The extra phase accumulated by the electron becomes a pure boundary term:

$$\Delta\phi_{\mathcal{B}} = -\kappa \left[\Delta V(T) - \Delta V(0)\right], \tag{3}$$

where $\Delta V(t) = V_1(t) - V_2(t)$ is the potential difference in volts and κ is a free parameter of dimension V^{-1}. For sinusoidal modulation $\Delta V(t) = \Delta V_0 \cos(\omega T)$ this yields a $1 - \cos(\omega T)$ contribution, functionally orthogonal to the standard $\sin(\omega T)$ AB phase.

The article is organised as follows. Section 2 formulates the phenomenological phase shift without reference to a specific microscopic Hamiltonian. Section 3 reviews the shielded electric AB configuration. Section 4 combines the two contributions and discusses their functional orthogonality. Section 5 describes a realistic electron interferometry experiment, estimates the sensitivity and analyses fringe-field systematics. Section 6 discusses the implications of either outcome, the absence of competitive existing bounds, and the broader epistemological stakes. Appendix Appendix A provides an analytical treatment of fringe-field phase shifts.

2. Phenomenological scalar phase

We consider the possibility that the scalar quantity $\mathcal{B} = \partial_\mu A^\mu$ has physical significance and couples weakly to electrons. Because the coupling is assumed to be perturbatively small, the electromagnetic fields inside the shielded cylinders are still described by Maxwell's equations to leading order. Hence $\mathbf{E} = \mathbf{B} = 0$ and $\mathcal{B} = \dot{\Phi}/c^2$. The most general phase shift compatible with linearity, temporal locality, and the static limit ($\dot{\Phi} = 0 \Rightarrow \Delta\phi = 0$) is a boundary term depending only on the initial and final values of the applied voltage:

$$\Delta\phi_{\mathcal{B}} = -\kappa \left[\Delta V(T) - \Delta V(0)\right]. \tag{4}$$

Here $\Delta V(t) = V_1(t) - V_2(t)$ is the potential difference in volts and κ is a phenomenological constant of dimension V^{-1} that quantifies the strength of the hypothetical coupling. No specific microscopic origin is assumed; κ is the single free parameter to be constrained by the experiment. This formulation avoids any dependence on a particular high-energy completion and makes the experimental search model-independent. (Although we remain agnostic about the ultraviolet completion, such a coupling arises naturally in emergent gauge theories [7,8], where exact gauge symmetry is only approximate and operators depending on $\partial_\mu A^\mu$ appear in the low-energy effective action.)

3. The shielded electric Aharonov-Bohm configuration

The geometry follows the original proposal [9]: two hollow cylindrical conductors of length L and inner radius R are placed along the two arms of an electron interferometer. Time-dependent voltages $V_1(t)$ and $V_2(t)$ are applied to their inner surfaces. For a perfect conductor in Maxwell electrodynamics, the interior electric field must vanish; the Laplace equation with Dirichlet boundary conditions has the unique solution $\Phi(\mathbf{r}, t) = V_j(t)$ throughout the volume. The vector potential can be chosen to vanish inside, so that $\mathbf{E} = \mathbf{B} = 0$ along the entire electron trajectory. The electron experiences no Lorentz force, yet its wave function accumulates the standard phase

$$\Delta\phi_{\mathrm{QM}} = -\frac{e}{\hbar}\int_0^T \Delta V(t)\,dt. \tag{5}$$

For a sinusoidal modulation $\Delta V(t) = \Delta V_0 \cos(\omega t)$,

$$\Delta\phi_{\mathrm{QM}} = -\frac{e\Delta V_0}{\hbar\omega}\,\sin(\omega T). \tag{6}$$

The transit time is $T = L/v$, with v the electron speed.

4. Scalar-mode signature and functional orthogonality

Adding the standard and scalar contributions, the total interferometric phase for sinusoidal modulation is

$$\Delta\phi(\omega T) = A\sin(\omega T) + C\left[1 - \cos(\omega T)\right], \tag{7}$$

with $A = -e\Delta V_0/(\hbar\omega)$ and $C = \kappa\Delta V_0$. The functional characteristics of the two terms are summarised in Table 1. They are linearly independent over any interval; their zero crossings are interleaved, enabling a clean separation by fitting a two-parameter model to data taken over a range of ωT values.

5. Experimental design and sensitivity

5.1. *Interferometer layout*

The apparatus (Fig. 1) employs a cold field-emission source, a biprism beam splitter, two shielded cylindrical electrodes ($L = 1$ cm, $R = 100$ μm, reducible to 10 μm), and a microchannel-plate detector. Two phase-locked RF synthesizers drive the

Table 1. Functional comparison of the standard and scalar phase contributions for $\Delta V(t) = \Delta V_0 \cos(\omega t)$.

Feature	**Standard QM**	**Scalar coupling**
Static limit ($\omega = 0$)	$\propto T$	0
Low-ωT scaling	Linear in T	$\propto (\omega T)^2$
Functional form	$\sin(\omega T)$	$1 - \cos(\omega T)$
Zeros	$\omega T = n\pi$	$\omega T = 2n\pi$
Maxima	$\omega T = (2n+1)\pi/2$	$\omega T = (2n+1)\pi$

cylinders with the same frequency ω but a controlled phase offset to produce the desired $\Delta V(t)$. Guard electrodes and a common Faraday cage suppress crosstalk. Electron energies between 10 eV and 10 keV give transit times T from 5.3 ns to 0.17 ns, corresponding to RF frequencies from $\sim$ 30 MHz to $\sim$ 3 GHz for a full ωT sweep. Single-electron interferometry with the required temporal resolution and phase stability has been demonstrated [12,11]. The setup thus constitutes a **high-precision quantum probe** for feeble time-dependent potentials, exploiting the Aharonov-Bohm phase as a transduction mechanism.

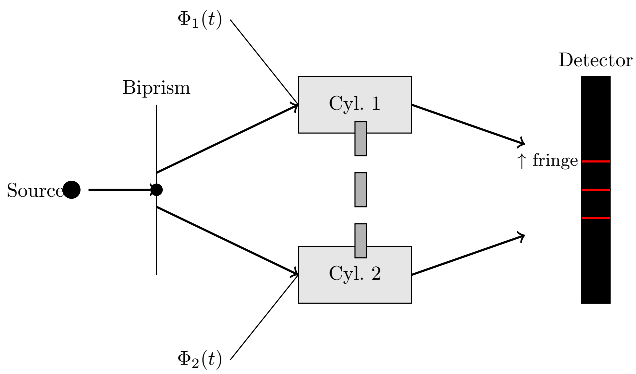

Fig. 1. Schematic of the electron interferometer. Two shielded cylindrical electrodes are driven by independent, phase-locked RF sources. Guard electrodes minimise crosstalk.

5.2. *Fringe-field systematics*

The fringe fields at the cylinder ends produce a spurious phase that must be carefully modelled. A detailed analytical treatment is given in Appendix Appendix A. The key result is that for cylinder radii $R \ll L$ and adiabatic traversal $\omega R/v \ll 1$, the fringe contribution takes the form

$$\Delta\phi_{\text{fringe}} = -\alpha \frac{e\Delta V_0}{\hbar} \frac{R}{v} \left[1 + \cos(\omega T)\right], \tag{8}$$

with $\alpha \sim \mathcal{O}(1)$. Its functional form $1 + \cos(\omega T)$ is orthogonal to both the standard and scalar terms, so it can be fitted simultaneously. The relative amplitude compared to the standard phase is $\sim \omega T\, R/L$, which for the proposed parameters remains below 0.03 when $R/L = 10^{-3}$. Additional systematic effects (finite conductivity, cavity resonances, beam energy spread) are discussed in the Appendix and are estimated to contribute at the 10^{-3} rad level or below after suitable mitigation.

5.3. *Projected sensitivity*

With a modulation amplitude $\Delta V_0 = 10$ V (easily generated by standard RF amplifiers) and an integrated electron count of $N = 10^{10}$ per frequency point, the shot-noise-limited phase resolution is $\delta\phi \approx N^{-1/2} = 10^{-5}$ rad. Reaching this level in practice requires exceptional interferometric stability; state-of-the-art single-electron interferometry has recently demonstrated phase resolutions of 10^{-4} rad [12], and the additional order of magnitude improvement is challenging but within reach with longer integration and active vibration control. If achieved, the minimal detectable scalar amplitude $|C| = \delta\phi$ yields a sensitivity to the coupling

$$|\kappa|_{\min} \approx \frac{\delta\phi}{\Delta V_0} \approx 10^{-6}\ \mathrm{V}^{-1}. \tag{9}$$

Even a more conservative resolution of 10^{-4} rad would still provide the first direct constraint on κ at the 10^{-5} V^{-1} level, which is entirely unconstrained at present.

6. Discussion

6.1. *Absence of existing competitive bounds*

No existing precision measurement constrains the coupling κ in a competitive manner. The electron anomalous magnetic moment [10], the Lamb shift, and DC voltage standards all involve static electric fields where $\mathcal{B} = 0$, and are therefore completely insensitive. The magnetic AB effect involves $\Phi = 0$ and $\nabla \cdot \mathbf{A} = 0$ outside the solenoid, so $\mathcal{B} = 0$ there as well.

The AC Josephson effect could in principle produce a boundary term proportional to κ during transients, but the accompanying standard Josephson phase is $\sim 10^{15}$ rad for a 1 V transient, while the scalar phase is $\sim \kappa \cdot 1$ V. For the scalar term to compete, κ would need to be $\sim 10^{15}$ V^{-1}, many orders of magnitude above our projected sensitivity [15]. Torsion-balance searches for fifth forces [13,14] probe static, gradient-driven potentials and are insensitive to a time-derivative coupling. Hence the proposed experiment would be the first to explore this parameter space.

6.2. *Scale of new physics – an indicative estimate*

If the scalar coupling originates from an effective operator $\frac{g}{\Lambda}\,\bar{\psi}\psi\,\partial_\mu A^\mu$ (with g a dimensionless coefficient of order unity and Λ a heavy mass scale), the phenomenological constant is $\kappa = ge/(\hbar\Lambda c^2)$. In natural units this corresponds to $\Lambda \sim ge/\kappa$, which for $|\kappa| = 10^{-6}$ V^{-1} gives $\Lambda \sim 1.7\,g$ GeV. Table 2 collects the values of κ for a range of Λ, assuming $g = 1$. It must be stressed that this conversion is purely indicative—it depends on the specific ultraviolet completion and on the assumption that the effective operator dominates. Nevertheless, it illustrates that a table-top electron interferometer can, in principle, probe energy scales comparable to those of high-energy physics, starting from the GeV domain and extending upward if $g < 1$.

Table 2. Effective coupling κ (for $g = 1$) as a function of the new-physics scale Λ. The values are indicative and depend on the assumed effective operator.

Λ	κ (V^{-1})
1 meV	1.7×10^{6}
1 eV	1.7×10^{3}
1 keV	1.7
1 MeV	1.7×10^{-3}
1 GeV	1.7×10^{-6}
1 TeV	1.7×10^{-9}

6.3. *Interpretation of a null result versus a positive signal*

A null result, establishing $|\kappa| \lesssim 10^{-6}$ V^{-1} (or 10^{-5} V^{-1} under conservative assumptions), would provide the first direct experimental evidence that the Lorenz condition reflects an exact dynamical decoupling: even in the field-free, time-dependent regime, the scalar mode does not interact with matter. This would elevate the gauge principle from a pragmatic recipe to an empirically verified constraint on the structure of electrodynamics.

A positive detection of a non-zero C would be equally foundational. It would reveal that the electromagnetic field possesses a third physical degree of freedom beyond the two transverse photon polarizations—a scalar mode that the standard formalism discards by fiat. Such a result would resonate with any theoretical framework in which the Lorenz condition is not a fundamental requirement, and would open a new chapter in the understanding of gauge symmetries.

6.4. *Epistemological context*

The history of physics provides examples of symmetries that were long considered inviolable until direct tests in new regimes revealed their limitations—parity violation in weak interactions being the paradigmatic case [16,17]. Gauge invariance has never been directly tested in a configuration where the fields vanish and only the potentials vary in time. The experiment proposed here would subject this foundational principle to its first empirical scrutiny in such a regime, independently of the underlying theoretical interpretation.

7. Conclusion

We have argued that the time-dependent electric Aharonov-Bohm effect is not merely the last unverified prediction of the 1959 AB paper, but also a uniquely clean **quantum probe** of the scalar sector of electrodynamics. By adopting a purely phenomenological approach, we have shown that a weak scalar coupling leads to a phase shift $\Delta\phi \propto \Delta V(T) - \Delta V(0)$, functionally orthogonal to the standard AB phase. A realistic electron interferometry experiment can reach a coupling sensitivity $|\kappa| \sim 10^{-6}$ V^{-1}, which would be the first direct exploration of this parameter space. Neither outcome—null or positive—would be trivial; both would substantially deepen our understanding of the ontology of gauge potentials and the foundations of electrodynamics.

Appendix A. Analytical treatment of fringe-field phase shifts

In the interior of a long, hollow, perfectly conducting cylinder, the central region is screened from electric fields. However, at the open ends the potential varies rapidly from its uniform bulk value $\Phi(t)$ to the grounded potential outside. An electron traversing the cylinder experiences these fringe regions at entry and exit. We derive here the resulting spurious interferometric phase $\Delta\phi_{\text{fringe}}$ analytically and demonstrate that its functional form is orthogonal to both the standard and scalar signals, allowing a clean separation.

Appendix A.1. *Potential solution and fringe profile*

Consider a single cylindrical conductor of inner radius R and length L, with its axis along z. The ends at $z = \pm L/2$ are open and held at ground potential $V = 0$. The lateral surface is maintained at a time-dependent potential $V(t)$, which varies slowly compared to the electron transit time through the fringe. We may therefore solve the electrostatic problem for the potential $\phi(\mathbf{r})$ at an instantaneous value $\Phi = V(t)$ on the lateral boundary. Laplace's equation $\nabla^2\phi = 0$ holds throughout the interior [18].

For a cylinder of finite length with mixed boundary conditions, the exact solution can be expanded in Bessel-Fourier modes [18,9]. On the axis ($\rho = 0$), the potential takes the form

$$V(0,z) = \Phi \sum_{n=1}^{\infty} \frac{2}{k_n R\, J_1(k_n R)} \frac{\sinh\left[k_n(L/2 - |z|)\right]}{\sinh(k_n L/2)}, \tag{A.1}$$

where $k_n R$ are the positive zeros of the Bessel function J_0, i.e., $J_0(k_n R) = 0$. For $L \gg R$, far from the ends ($|z| \ll L/2$), the potential tends uniformly to Φ. Near an open end, e.g. $z \approx L/2$, the series is dominated by the first term $n = 1$, with $k_1 = \chi_{01}/R \approx 2.4048/R$. The potential decays exponentially towards zero over a characteristic length $\sim R$. We can thus model the fringe profile near one end with a smooth, normalised function $f(z/R)$ that transitions from 0 (outside) to 1 (deep inside). The exact shape is not critical; only its integral matters for the accumulated phase.

Appendix A.2. *Phase accumulation and adiabatic condition*

The fringe traversal time is $\tau_f \sim R/v$, where v is the electron speed. For the proposed parameters ($R \sim 10 - 100\ \mu$m, $v \sim 10^6 - 10^7$ m/s), $\tau_f \sim 10^{-12}$ s. If the modulation frequency satisfies $\omega\tau_f \ll 1$, the potential can be taken as constant during the fringe crossing. This adiabatic condition, $\omega R/v \ll 1$, is well satisfied: at our highest frequencies (~ 1 GHz) and lowest electron energies, $\omega R/v \lesssim 0.1$. Corrections to the adiabatic approximation are of order $(\omega R/v)^2 \lesssim 10^{-2}$ and can be safely neglected.

The electron accumulates a fringe phase at entry ($t \approx 0$) given by

$$\phi_{\text{entry}} = -\frac{e}{\hbar}\int_{-\infty}^{0} \Phi(0) f(z/R)\frac{dz}{v} = -\frac{e}{\hbar}\Phi(0)\frac{R}{v}I_f, \tag{A.2}$$

with the geometric integral $I_f = \int_{-\infty}^{\infty} f(u)\,du$. A similar contribution arises at the exit end ($t \approx T$) with instantaneous potential $\Phi(T)$. For the exponential decay governed by the first Bessel mode, numerical evaluation gives $I_f \approx 0.9$. We conservatively set the overall constant $\alpha = I_f \simeq 1$ in what follows.

Appendix A.3. *Interferometric phase difference and functional orthogonality*

Summing the contributions from both ends and taking the difference between the two interferometer arms, we obtain the fringe phase difference

$$\Delta\phi_{\text{fringe}} = -\alpha\frac{e}{\hbar}\frac{R}{v}\big[\Delta\Phi(0) + \Delta\Phi(T)\big], \tag{A.3}$$

where $\Delta\Phi(t) = \Phi_1(t) - \Phi_2(t)$. For the sinusoidal modulation $\Delta\Phi(t) = \Delta\Phi_0\cos(\omega t)$, this reduces to

$$\Delta\phi_{\text{fringe}} = -\alpha\frac{e\Delta\Phi_0}{\hbar}\frac{R}{v}\big[1 + \cos(\omega T)\big]. \tag{A.4}$$

The amplitude of this spurious signal is suppressed by a factor $\sim R/L$ relative to the standard AB phase, since $\frac{e\Delta\Phi_0}{\hbar}\frac{R}{v} \sim \frac{R}{L}\times\frac{e\Delta\Phi_0}{\hbar}T$. For the proposed geometry with $R/L \sim 10^{-3}$, the fringe amplitude is at most a few percent of the standard signal. Crucially, the functional form $1+\cos(\omega T)$ is linearly independent of both $\sin(\omega T)$ (standard phase) and $1-\cos(\omega T)$ (scalar phase). A simultaneous three-parameter fit

$$\Delta\phi(\omega T) = A\sin(\omega T) + C[1 - \cos(\omega T)] + F[1 + \cos(\omega T)] \tag{A.5}$$

to data spanning a sufficient range of ωT (e.g., 0.2π to 10π) can extract all three amplitudes without degeneracy. Small uncertainties in the exact value of α (due to geometric tolerances or slight beam misalignment) do not affect the shape of the fringe term, only its fitted coefficient F. The scalar amplitude C remains robustly identifiable by its distinct functional dependence. This confirms that fringe fields do not constitute a fundamental obstacle to the proposed measurement.

Appendix A.4. *Additional systematic considerations*

Finite conductivity of the cylinder walls introduces a small penetration depth $\delta \ll R$, which modifies the fringe profile at the level of $\delta/R \lesssim 10^{-3}$ for copper at GHz frequencies [18]. Cavity resonances inside the cylinders can be avoided by keeping the cylinder length below the cutoff wavelength for the lowest TM mode, which is satisfied for $L = 1$ cm at the operating frequencies. The energy spread of the electron beam ($\Delta E/E \sim 10^{-4}$ for a cold field emitter) translates into a spread in transit time $\Delta T/T \approx \frac{1}{2}\Delta E/E$, which, for the highest $\omega T \sim 10\pi$, gives a phase smearing of order 10^{-3} rad. All these effects are well below the projected sensitivity and can be further mitigated with standard techniques.

Author Declarations

Conflict of interest

The authors have no conflicts to disclose.

Data Availability

Data sharing is not applicable to this article as no new data were created or analyzed in this study.

References

1. Y. Aharonov and D. Bohm, "Significance of electromagnetic potentials in the quantum theory," *Phys. Rev.* **115**, 485–491 (1959).
2. A. Tonomura, T. Matsuda, R. Suzuki, A. Fukuhara, N. Osakabe, H. Umezaki, J. Endo, K. Shinagawa, Y. Sugita, and H. Fujiwara, "Observation of Aharonov-Bohm effect by electron holography," *Phys. Rev. Lett.* **48**, 1443–1446 (1982).
3. R. A. Webb, S. Washburn, C. P. Umbach, and R. B. Laibowitz, "Observation of h/e Aharonov-Bohm oscillations in normal-metal rings," *Phys. Rev. Lett.* **54**, 2696–2699 (1985).
4. H. Batelaan and A. Tonomura, "The Aharonov-Bohm effects: Variations on a subtle theme," *Phys. Today* **62**(9), 38–43 (2009).
5. G. Matteucci and G. Pozzi, "New diffraction experiment on the electrostatic Aharonov-Bohm effect," *Phys. Rev. Lett.* **54**, 2469–2472 (1985).
6. S. A. Hilbert, B. Barwick, M. Fabrikant, C. J. G. J. Uiterwaal, and H. Batelaan, "Experimental observation of time-delays associated with electric Matteucci-Pozzi phase shifts," *New J. Phys.* **13**, 093025 (2011).
7. X.-G. Wen, *Quantum Field Theory of Many-Body Systems* (Oxford University Press, Oxford, 2004).
8. M. Levin and X.-G. Wen, "Colloquium: Photons and electrons as emergent phenomena," *Rev. Mod. Phys.* **77**, 871–879 (2005).
9. M. Peshkin and A. Tonomura, *The Aharonov-Bohm Effect* (Lecture Notes in Physics, Vol. 340), Springer, Berlin (1989).
10. D. Hanneke, S. Fogwell, and G. Gabrielse, "New measurement of the electron magnetic moment and the fine structure constant," *Phys. Rev. Lett.* **100**, 120801 (2008).

11. F. Hasselbach, “Progress in electron- and ion-interferometry,” *Rep. Prog. Phys.* **73**, 016101 (2010).
12. H. Bartolomei, E. Frigerio, M. Ruelle, G. Rebora, Y. Jin, U. Gennser, A. Cavanna, E. Baudin, J.-M. Berroir, I. Safi, P. Degiovanni, G. C. Ménard, and G. Fève, “Time-resolved sensing of electromagnetic fields with single-electron interferometry,” *Nat. Nanotechnol.* (2025), doi:10.1038/s41565-025-01899-3.
13. E. G. Adelberger, B. R. Heckel, and A. E. Nelson, “Tests of the gravitational inverse-square law,” *Annu. Rev. Nucl. Part. Sci.* **53**, 77–121 (2003).
14. E. Fischbach and C. L. Talmadge, *The Search for Non-Newtonian Gravity* (Springer, New York, 1999).
15. M. Tinkham, *Introduction to Superconductivity*, 2nd ed. (Dover, New York, 2004).
16. T. D. Lee and C. N. Yang, “Question of Parity Conservation in Weak Interactions,” *Phys. Rev.* **104**, 254–258 (1956).
17. C. S. Wu, E. Ambler, R. W. Hayward, D. D. Hoppes, and R. P. Hudson, “Experimental Test of Parity Conservation in Beta Decay,” *Phys. Rev.* **105**, 1413–1415 (1957).
18. J. D. Jackson, *Classical Electrodynamics*, 3rd ed. (Wiley, New York, 1999).